A NOVEL HIGH-PRECISION SPECTRAL DECOMPOSITION METHOD BASED ON SECOND-ORDER SYNCHROSQUEEZING TRANSFORM AND ITS APPLICATION

ZHIWEI GUO and SIYUAN CAO

State Key Laboratory of Petroleum Resources and Engineering, CNPC Key Laboratory of Geophysical Exploration, China University of Petroleum (Beijing), 18 Fuxue Road, Changping, Beijing 102249, P.R. China. zhiwei_cupb@126.com; csy@cup.edu.cn

ABSTRACT

Guo, Z.W. and Cao, S.Y., 2020. A novel high-precision spectral decomposition method based on second-order synchrosqueezing transform and its application. *Journal of Seismic Exploration*: 29, 159-172.

Spectral decomposition plays a central role in characterizing multicomponent signals, as for instance seismic signal, because it can reveals lots of valuable information hidden in the broadband seismic response. This paper presents a new methodology for seismic spectral decomposition via second-order synchrosqueezing transform. Second-order synchrosqueezing transform, which relies on a second-order local estimate of the instantaneous frequency, can provide a sharpened time-frequency representation while allowing for the separation and the reconstruction of the modes. We validate our method by means of a synthetic model and compare with the conventional spectral decomposition algorithms. Two field examples are employed to illustrate that the seismic attributes delineation using the second-order synchrosqueezing transform based method gives a better reflection of hydrocarbon-saturated reservoirs and stratigraphic characteristics.

KEY WORDS: spectral decomposition, second-order synchrosqueezing transform, seismic signal, hydrocarbon detection, stratigraphic characteristics.

INTRODUCTION

Spectral decomposition is considered as a key tool suited for analyzing non-stationary signals whose frequency content changes with time and has been very commonly applied in geophysical exploration, for example, seismic thin bed analysis (Partyka et al., 1999), reservoir characterization (Chen et al., 2014; Radad et al., 2016), ground-roll elimination (Liu and Fomel, 2013; Liu et al., 2016), hydrocarbon indentification (Castagna et al.,

2003; Farfour et al., 2013; Chen et al., 2014) and channel sands detection (Odebeatu et al., 2006; Wu et al., 2014). Over the last decade, numerous methods have been proposed for spectral decomposition. One of the most powerful approaches developed is probably short time Fourier transform (STFT), which achieves a localized time-frequency representation based on the windowed Fourier transform (Allen, 1977). Unfortunately, its time-frequency resolution is intrinsically influenced by the window size. The continuous wavelet transform (CWT) stems from the fact that STFT is associated with a fixed time and frequency resolution because the length of the analysis window remains unchanged. In fact, CWT leads to good time resolution for high-frequency events and good frequency resolution for low-frequency events (Rioul et al., 1991; Sinh et al., 2005). However, CWT suffers from an intrinsic limitation known as the uncertainty principle, which stipulates that one cannot localize a signal with an arbitrary precision both in time and frequency. Many attempts have been made to deal with this problem, such as Wigner-Ville distribution (WVD) (Jeffrey, 1999) and Cohen distribution (Cohen, 1966). The former belongs to quadratic time-frequency methods; the latter is a special case of which being squared STFT. Although offering a dramatic improvement in terms of time-frequency resolution, the existence of cross-term interference limits the time-frequency readability of seismic signals. The reassignment method (RM) is a general methodology to sharpen time-frequency representations in a somehow restricted framework (Kodera, 1976). It, however, faces with the disadvantage that the reassigned transform is no longer invertible. In 2011, Daubechies and Maes proposed another phase based technique, called synchrosqueezing transform (SST), its purpose is also to sharpen the time-scale representation given by CWT. Meanwhile, the SST is an adaptive and invertible transform that improves the readability of a wavelet-based time-frequency map (Li and Liang, 2012). Originally proposed as a post-processing method applied to CWT, SST can alternatively be applied to STFT with minor changes, to obtain the so-called STFT-based SST (FSST) (Thakur and Wu, 2011; Oberlin et al., 2014). However, the applicability of FSST is somewhat limited by the requirement of weak frequency modulation hypothesis for the modes constituting the signal. To deal with this issue, an extension of FSST to the context of strongly modulated modes, called second-order synchrosqueezing transform (FSST2), was proposed by Oberlin (Oberlin et al., 2015), which relies on a second-order local estimate of the instantaneous frequency to improve modes localization and reconstruction.

In this paper, we extend our study for seismic spectral decomposition based on FSST2, which enables not only to obtain a highly concentrated time-frequency representation, but also to allow for the mode retrieval with a reasonable precision. The outline of the paper is as follow: in Section 2, we introduce the fundamental concept and theory of FSST2. We then employ a synthetic example to put the emphasis on the outstanding performance in sharpening time-frequency map compared with FSST. Section 4 is devoted to the presentation of two field datasets, which further demonstrate the potential of FSST2 in detecting hydrocarbon-saturated reservoirs and depicting stratigraphic characteristics.

SECOND-ORDER SYNCHROSQUEEZING TRANSFORM

The second-order STFT-based synchrosqueezing transform (FSST2), an adaptation of STFT-based SST (FSST), is capable of sharpening the time-frequency representation of a signal while allowing for the separation and retrieval of the modes.

An AM-FM signal is expressed as follows:

$$f(\tau) = A(\tau)e^{i2\pi\phi(\tau)} \;, \tag{1}$$

where $A(\tau)$ and $\phi(\tau)$ are respectively the instantaneous amplitude and phase functions.

The short-time Fourier transform (STFT) of signal f, with respect to the window g, can be represented via the following formula:

$$V_f^g(t,\eta) = \int f(\tau)g^*(\tau-t)e^{-i2\pi\eta(\tau-t)}d\tau \;, \tag{2}$$

where g^* is the complex conjugate of g.

The conventional FSST is defined by:

$$T_f^{g,\gamma}(t,\omega) =$$
$$\frac{1}{g^*(0)}\int_{\{\eta,|V_f^g(t,\eta)|>\gamma\}}V_f^g(t,\eta)\delta(\omega-\omega_f(t,\eta))d\eta \;, \tag{3}$$

where γ stands for some threshold and δ denotes the Dirac distribution. $\omega_f(t,\eta)$ represents the estimated instantaneous frequency at time t and frequency η:

$$\omega_f(t,\eta) = R\left\{\frac{\partial_t V_f^g(t,\eta)}{i2\pi V_f^g(t,\eta)}\right\} \;, \tag{4}$$

where $R\{\bullet\}$ means the real part of complex number, and ∂_t is the partial derivative with respect to t.

The FSST2 is a new extension of FSST, which aims to improve modes localization and reconstruction and suit for a wide variety of signals by means of a second-order local estimate for the instantaneous frequency.

Given a signal f, the complex reassignment operator $\omega_f(t,\eta)$ and $\tau_f(t,\eta)$ are respectively defined as

$$\omega_f(t,\eta) = \frac{\partial_t V_f^g(t,\eta)}{i2\pi V_f^g(t,\eta)} \qquad , \tag{5}$$

$$\tau_f(t,\eta) = t - \frac{\partial_\eta V_f^g(t,\eta)}{i2\pi V_f^g(t,\eta)} \qquad . \tag{6}$$

Then, the second-order local complex instantaneous frequency is represented as:

$$\omega_{t,f}^{[2]}(t,\eta) = \begin{cases} \omega_f(t,\eta) + q_{t,f}(t,\eta)\left(t - \tau_f(t,\eta)\right) & \partial_t\tau_f \neq 0 \\ \omega_f(t,\eta) & otherwise \end{cases} \tag{7}$$

where

$$q_{t,f}(t,\eta) = \frac{\partial_t \omega_f(t,\eta)}{\partial_t \tau_f(t,\eta)} \quad \partial_t\tau_f(t,\eta) \neq 0 \quad . \tag{8}$$

Therefore, FSST2 can be obtained by simply replacing $\omega_f(t,\eta)$ by $\omega_{t,f}^{[2]}(t,\eta)$ in eq. (3).

$$T_{2,f}^{g,\gamma}(t,\omega) = \frac{1}{g^*(0)} \int_{\left\{\eta, \left|V_f^g(t,\eta)\right| > \gamma\right\}} V_f^g(t,\eta)\,\delta\left(\omega - \omega_{t,f}^{[2]}(t,\eta)\right)d\eta \tag{9}$$

Ultimately, the original signal f can be approximately reconstructed by integrating $T_{2,f}^{g,\gamma}(t,\omega)$ in the vicinity of the corresponding ridge $\left(t,\phi'(t)\right)$:

$$f(t) \approx \int_{\left\{\omega, \left|\omega - \varphi(t)\right| < d\right\}} T_{2,f}^{g,\gamma}(t,\omega)\,d\omega \qquad , \tag{10}$$

where is the compensation factor and $\varphi(t)$ is an estimate for $\phi'(t)$.

SYNTHETIC DATA

A synthetic signal is employed to test the proposed method, which is a non-stationary multicomponent signal consisting of two modes and is shown as

$$s(t) = s_1(t) + s_2(t) \quad , \tag{11}$$

with

$$s_1(t) = 3\cos\left(2\pi\left(50t\right)\right) \quad 0 \le t < 1$$

$$s_2(t) = \begin{cases} 3\cos\left(2\pi\left(250t - 100t^2\right)\right) & 0 \le t < 0.5 \\ 3\cos\left(2\pi\left(250t - 200t^2 + \dfrac{400}{3}t^2 + \dfrac{1}{3}\right)\right) & 0.5 \le t < 1 \end{cases} \quad . \tag{12}$$

The original signal is displayed in Fig. 1, it is worth noting that $s_1(t)$ possesses a constant frequency, and the component $s_2(t)$ is the combination of a linear chirp signal and a quadratic chirp one. We use FSST and FSST2 to analyze the synthetic signal, respectively and the corresponding results are presented in Fig. 2. It can be observed that FSST generates some inaccuracy in the estimated instantaneous frequency, which results in energy diffusion in the time-frequency plane [Fig. 2(a)]. While in the case of FSST2, the energy gets obviously concentrated due to the estimation for instantaneous frequency with a high precision [Fig. 2(b)]. Meanwhile, the enlarged local time-frequency results from the rectangles in Fig. 2 further show the high resolutions in both time and frequency for FSST2 (Fig. 3), which is very beneficial to characteristics extraction for the non-stationary signal.
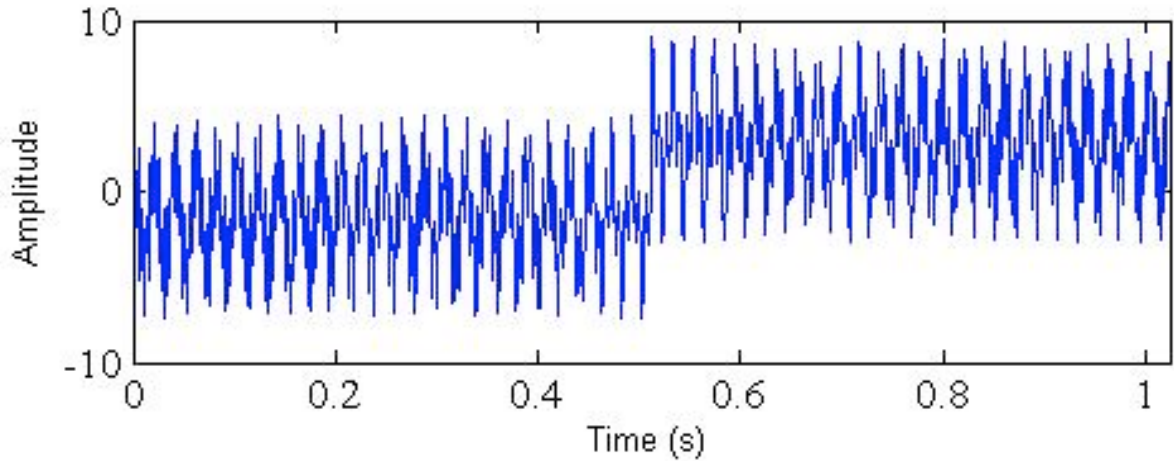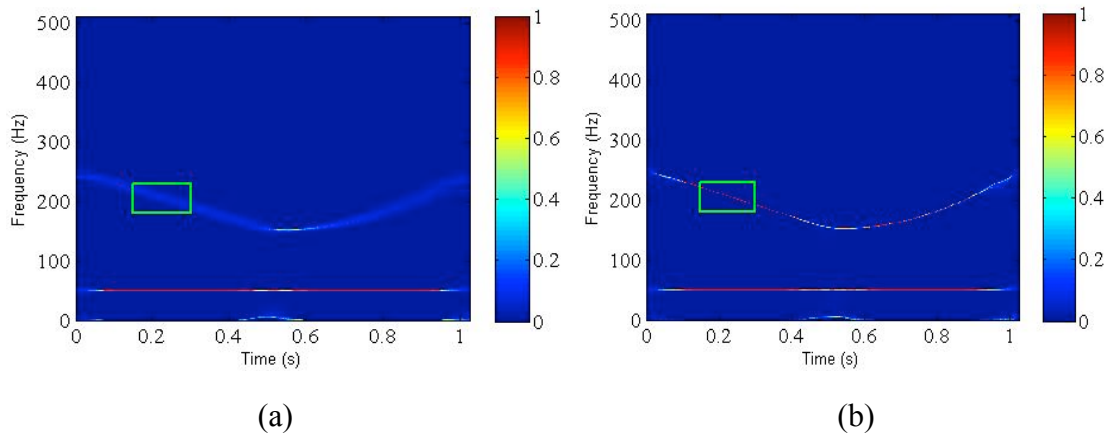

Fig. 1. Synthetic signal with two components.

(a)   (b)

Fig. 2. Time-frequency map obtained by FSST (a) and FSST2 (b), respectively. FSST2 shows a relatively sharp time-frequency map.

(a)   (b)
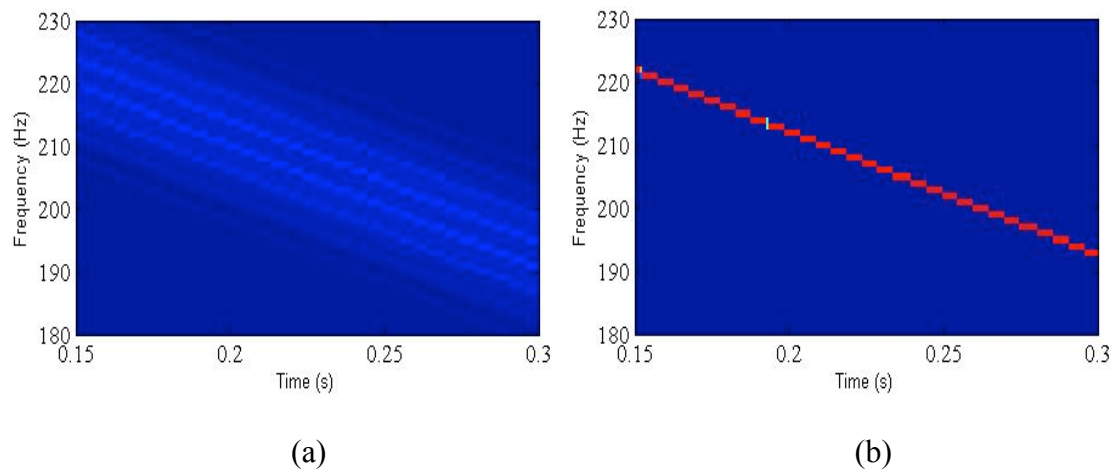
Fig. 3. Enlarged local time-frequency representation corresponding to Fig. 2. The energy is much more concentrated using FSST2 (b) than FSST (a).

FIELD EXAMPLES

Data Ⅰ

It is well known that the low-frequency anomalies associated with gas-charged reservoir have been utilized as a substantiating hydrocarbon indicator (Castagna et al., 2003). In this section, FSST2 is applied to analyze the gas-filled sand reservoir [Fig. 4(a)] to verify the effectiveness for detection of hydrocarbon. This dataset is comprised of 60 traces, the time range is from 3.5 s to 4.5 s and sampling period is 2 ms. The gas-filled area is indicated by the arrow and the trace 20, which passes through the reservoir, is shown in Fig. 4(b). Obviously, the strong amplitude locates in around 4s. The time-frequency representations obtained by FSST and FSST2 are demonstrated in Fig. 5. The FSST method has generated a blurred time-frequency map [Fig. 5(a)], which possibly dues to inaccuracy instantaneous frequency estimate. As for FSST2, it is capable of presenting the clearer time-frequency features of seismic signal and the higher time-frequency resolution.

Figs. 6(a) and 6(b) are the common frequency slices of 20 Hz and 40 Hz, respectively, obtained by using FSST-based method. The results with the same frequencies from the FSST2-based method are showed in Figs. 6(c) and 6(d), respectively. As we seen from Fig. 6, both methods exhibit the similar characteristics, in other words, the low-frequency anomaly is obvious near the gas-bearing reservoir at 20 Hz, and then the energy is attenuated at 40 Hz. However, FSST2 provides the higher time-frequency resolution than FSST-based method, which is helpful in depicting the location and extent of the gas-charged sand reservoir more precisely. In addition, the energy from 20 Hz to 40 Hz is attenuated more dramatically and the variations in amplitude are clearer for FSST2, that is to say, the FSST2-based method is more sensitive to gas-filled reservoir and is more suited for low frequency anomaly detection associated with hydrocarbon.

(a)

(b)
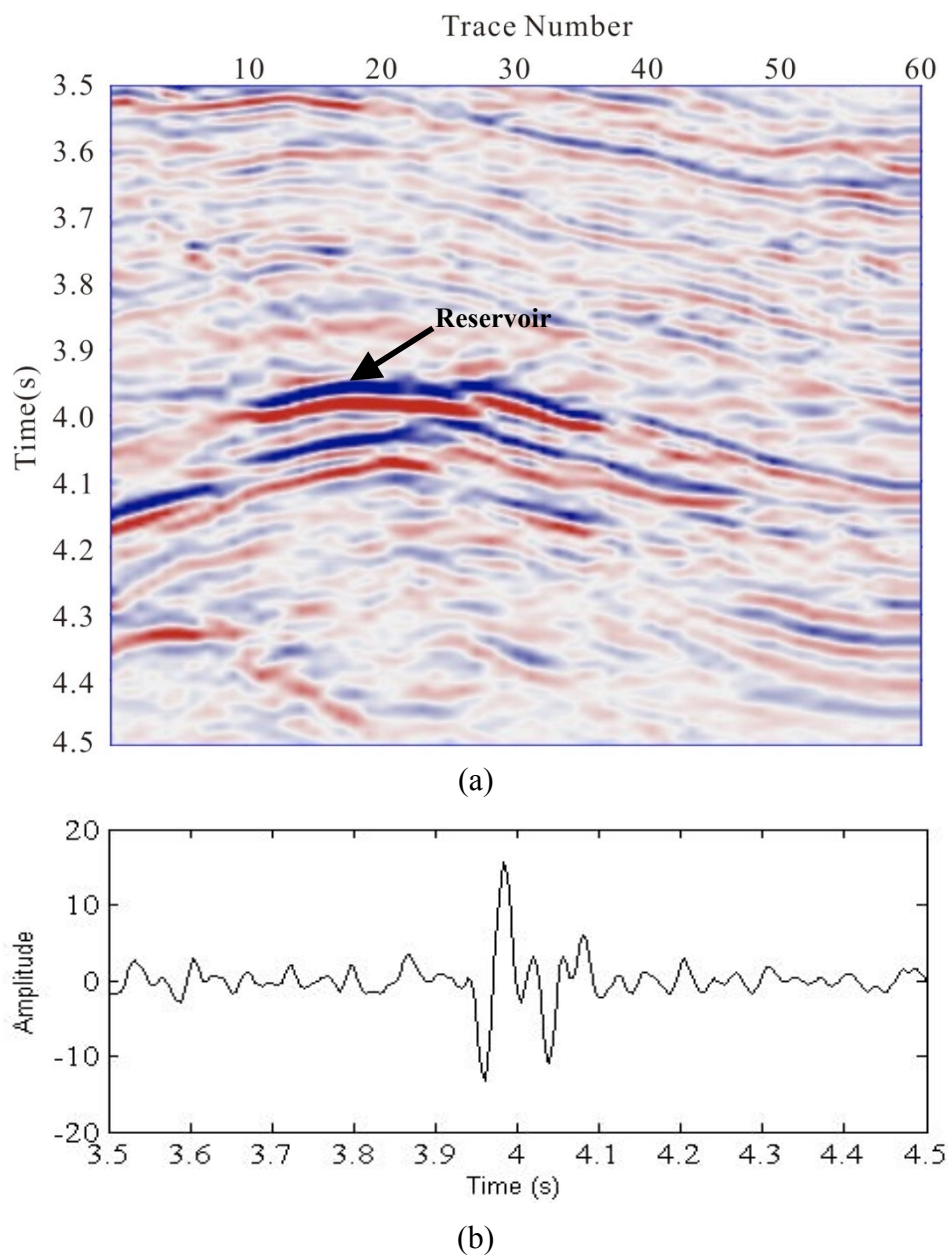
Fig. 4. The real post-stack data (a) and the corresponding trace 20. The arrow indicates a gas-charged reservoir and the trace 20 is characterized by strong amplitude around 4s.
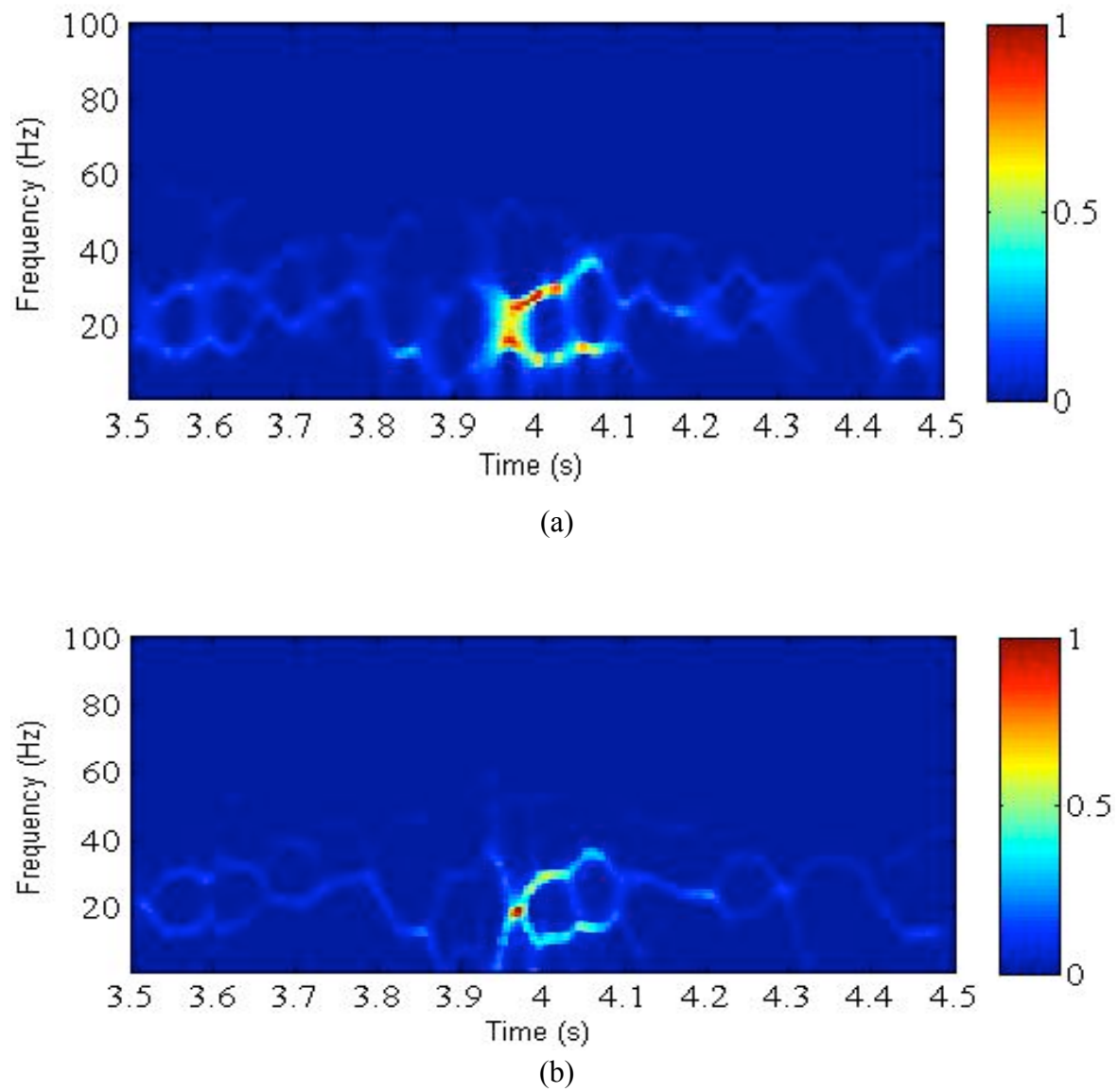
(a)

(b)

Fig. 5. The time-frequency map of trace 20 obtained by FSST (a) and FSST2 (b).
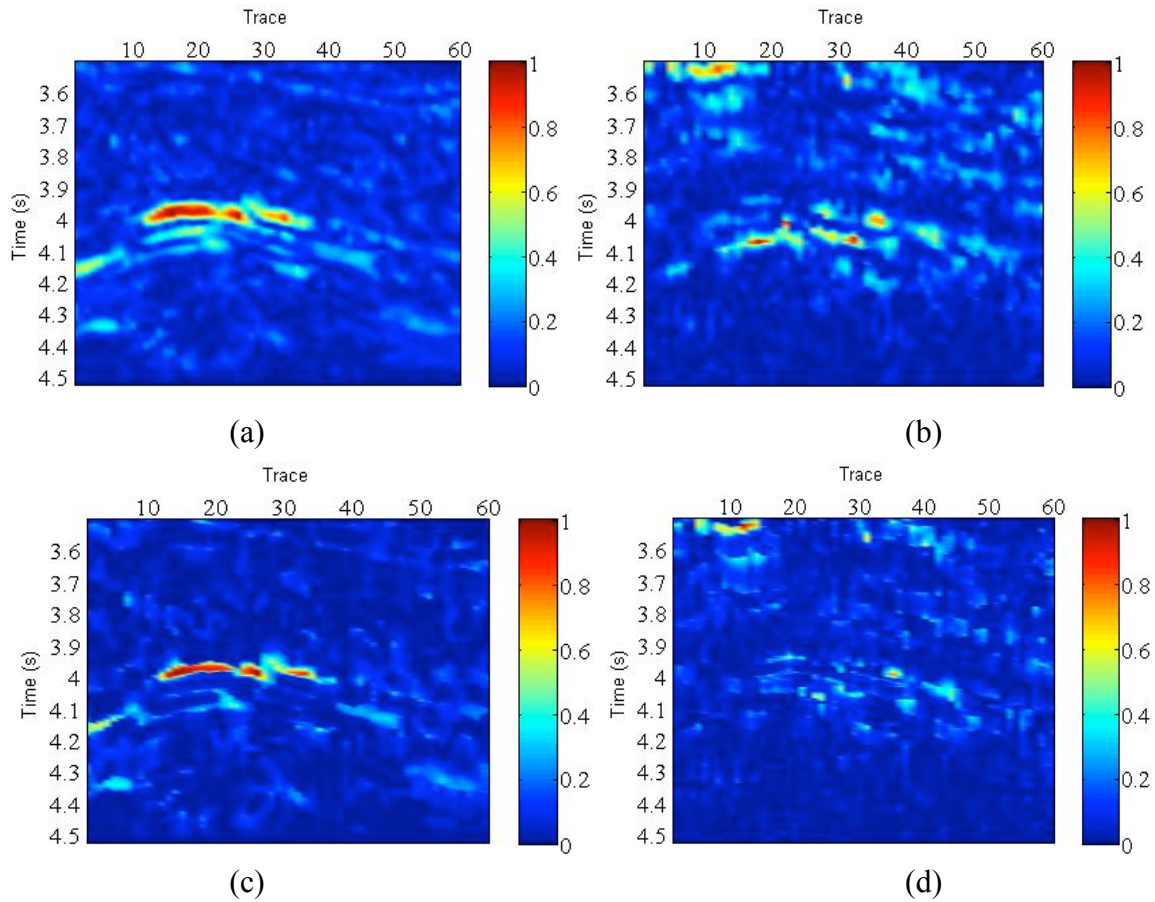
Fig. 6. (a) and (b) are the frequency slices of 20 Hz and 40 Hz, using FSST-based method. (c) and (d) are the same frequency slices, using FSST2-based method. FSST2 displays the higher frequency resolution compared with FSST; the variations in energy from 20 Hz to 40 Hz are clearer, and which is reduced rapidly.

Data Ⅱ

Further validation of the potential for FSST2 to delineate stratigraphic characteristics, we perform FSST2 on another seismic data [Fig. 7(a)] and extract the spectral slices (Fig. 9). For comparison, the FSST is also implemented to the same data. Fig. 7(b) is trace 170, which stems from the original post-stack section [Fig. 7(a)]. Time-frequency representations of trace 170 obtained by FSST and FSST2 are shown in Figs. 8(a) and 8(b), respectively. It can be obviously observed that FSST2 can effectively improve the energy concentration of time-frequency map compared with FSST and the time-frequency curves is more clear, so that more precise spectral anomalies can be captured by analyzing time-frequency representation.
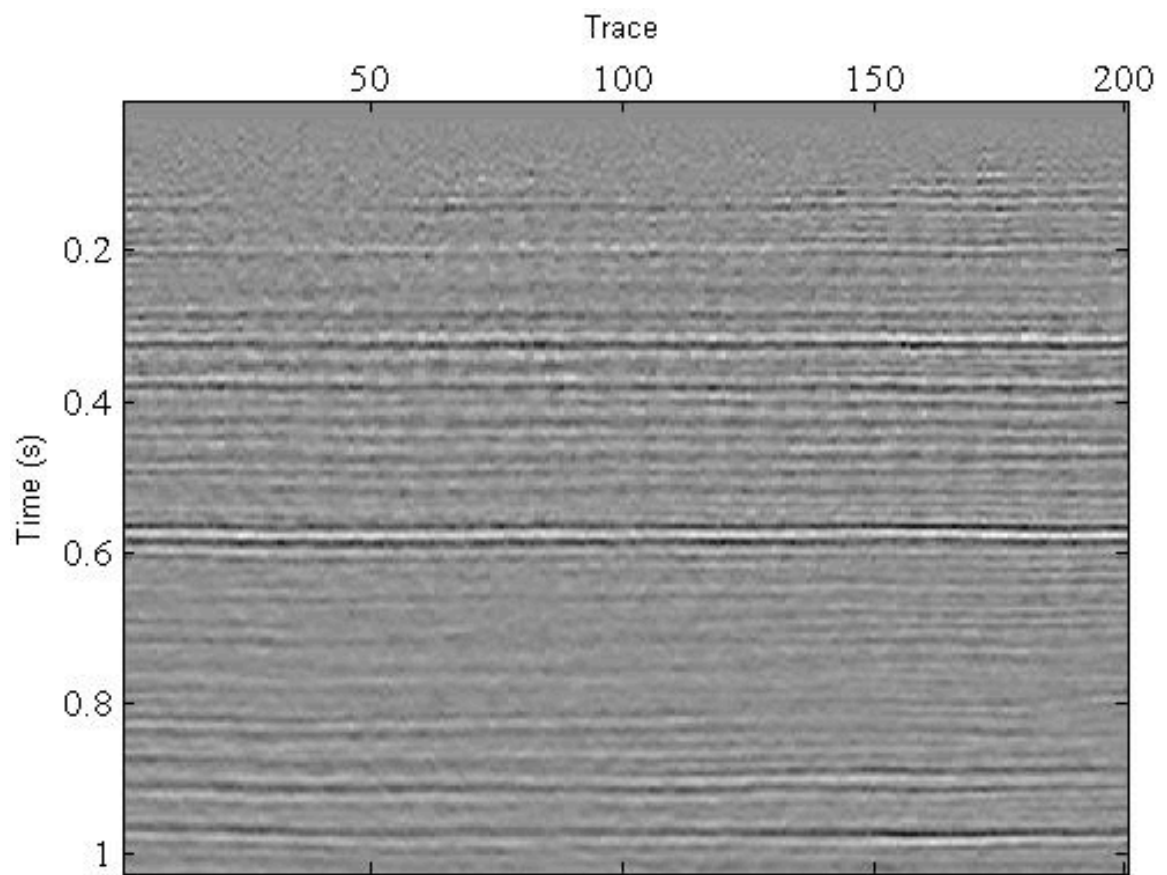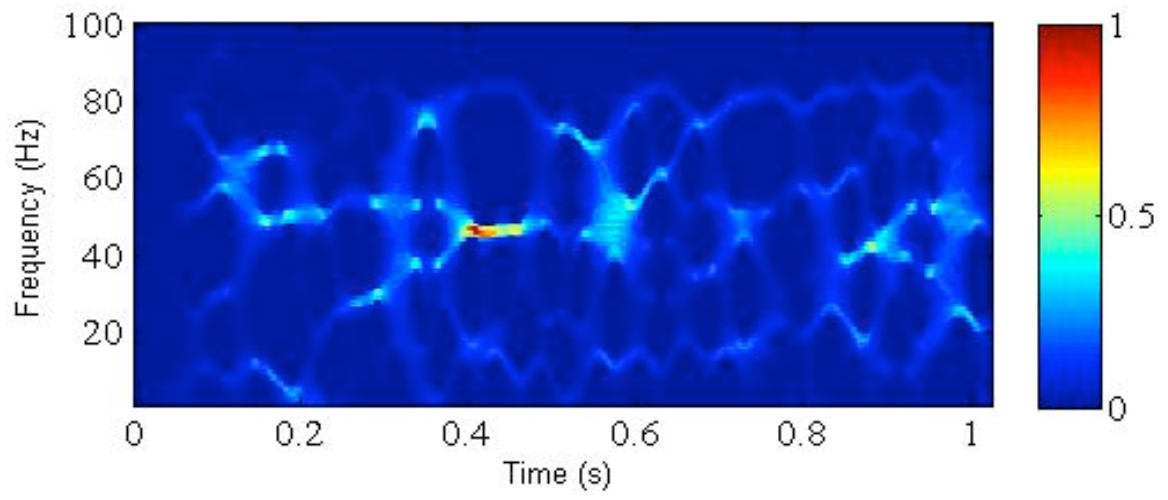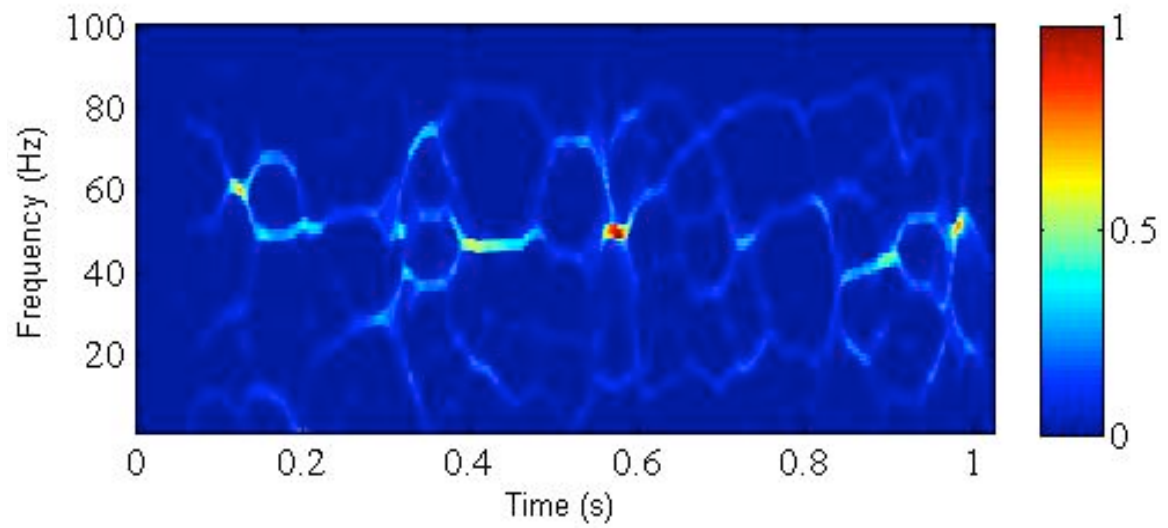
(a)
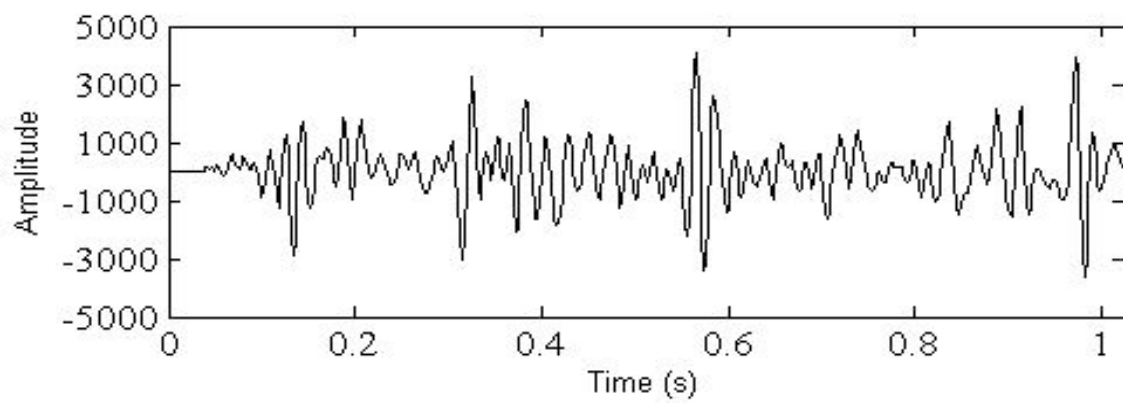
(b)

Fig. 7. A field data (a) and trace 170 (b).

(a)

(b)

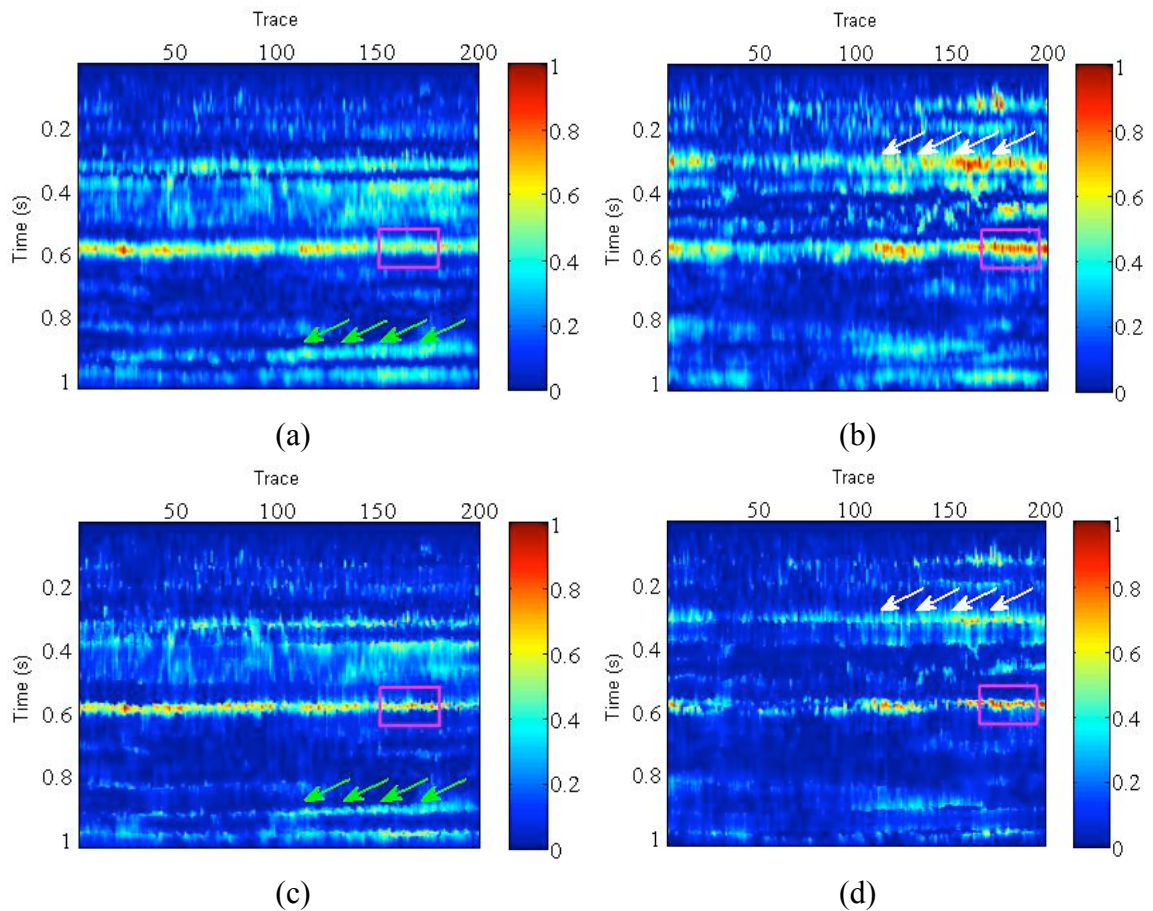Fig. 8.   The time-frequency representation of trace 170 generated by FSST (a) and FSST2 (b).

Fig. 9. Constant frequency slices. 40Hz obtained by using (a) FSST-based and (c) FSST2-based. 55Hz extracted by using (b) FSST-based and (d) FSST2-based.

Figs. 9(a) and 9(b) show the constant frequency slices of 40Hz and 55Hz for FSST. The results from FSST2-based method are displayed in Figs. 9(c) and 9(d), corresponding to 40 Hz and 55 Hz, respectively. We can find that both methods effectively extract stratigraphic characteristics, however, The FSST gives the blurred spectral slices [Figs. 9(a) and 9(b)], which makes the seismic interpretation more difficult (marked by the arrows). While the FSST2-based method exhibits more clearly spectral attributes and the variations in energy from 40 Hz to 55 Hz are very obvious, which helps to track the trend and extent of subsurface geologic structure. Besides, for further comparison, the zoom-in versions in the rectangles from Fig. 9 are plotted in Fig. 10. Notice the significant improvement in time-frequency map readability and spectrum resolution for FSST2 when compared with FSST, which facilitates the subsequent seismic processing and interpretation.
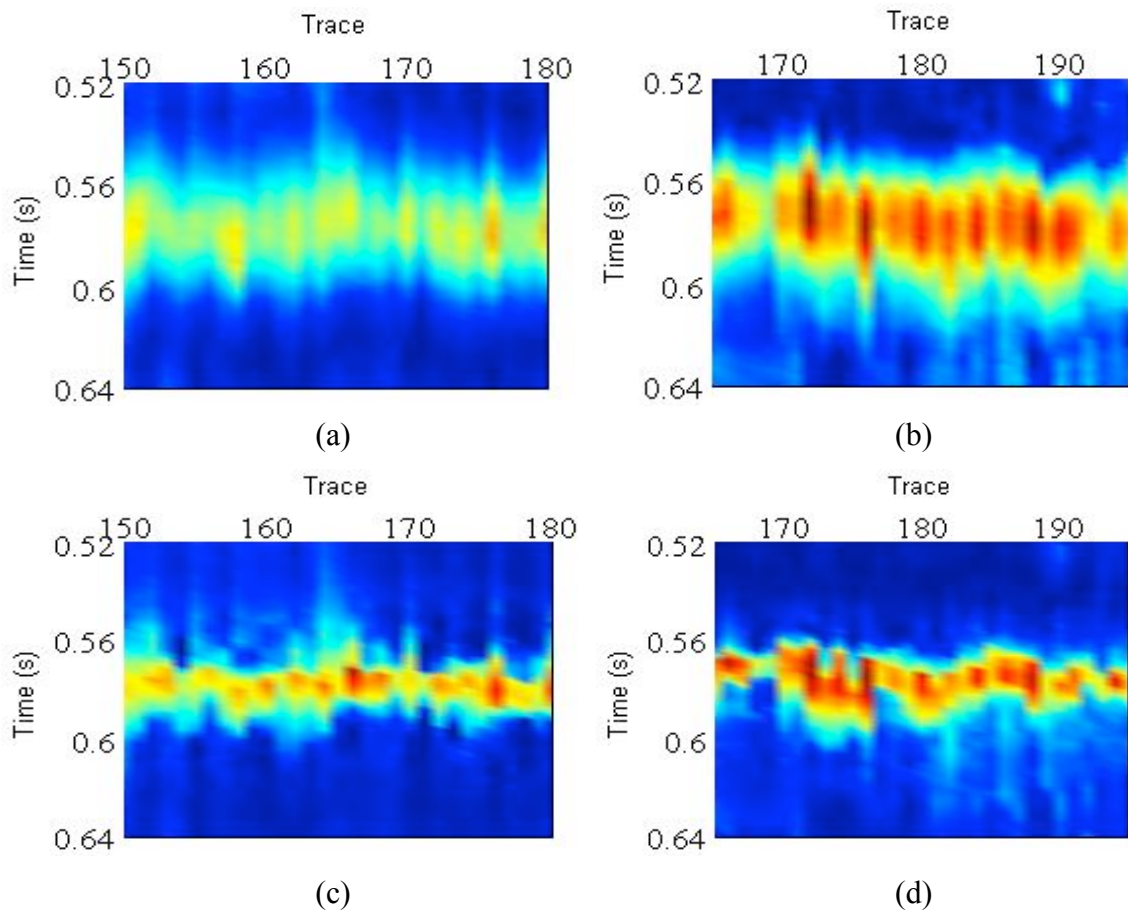
Fig. 10. The zoom-in version from the rectangles in Fig. 9. (a) 40 Hz FSST-based method, (b) 55 Hz FSST-based method, (c) 40 Hz FSST2-based method, (d) 55 Hz FSST2-based method.

CONCLUSIONS

In this study, a novel spectral decomposition based on second-order synchrosqueezing transform (FSST2) is proposed to analyze the non-stationary signal. FSST2 overcomes the diffusion of time-frequency map by introducing a second-order local estimate of the instantaneous frequency and provides time-frequency representation with more desirable energy concentration. The FSST2 is validated by a synthetic data and two field examples. On the one hand, FSST2 is more sensitive to hydrocarbon, which suits for the low frequency anomaly detection associated with gas-charged reservoir. On the other hand, the spectral frequency slices with higher resolution also demonstrate FSST2's potential in delineation of the subsurface geology structure and stratigraphic features, which renders that the FSST2 is promising for seismic data analysis.

ACKNOWLEDGEMENTS

REFERENCES

Allen, J.B., 1977. Short term spectral analysis, synthetic and modification by discrete Fourier transform. IEEE Transact. Acoust., Speech, Signal Process., 25: 235-238.

Castagna, J.P., Sun, S. and Siegfried, R.W., 2003. Instantaneous spectral analysis: detection of low-frequency shadows associated with hydrocarbons. The Leading Edge, 22: 120-127.

Chen, S., Li, X. and Wu, X., 2014, Application of frequency-dependent AVO inversion to hydrocarbon detection. J. Seismic Explor., 23: 241-264.

Chen, Y., Liu, T., Chen, X., Li, J. and Wang, E., 2014. Time-frequency analysis of seismic data using synchrosqueezing wavelet transform. J. Seismic Explor., 23: 303-312.

Cohen, L., 1966. Generalized phase-space distribution functions. J. Math. Phys., 7: 781-786.

Daubechies, I., Lu, J. and Wu, H.-T. W., 2011. Synchrosqueezed wavelet transform: An empirical mode decomposition-like tool. Appl. Comput. Harmon. Analis., 30: 243-261.

Farfour, M., Wang, J., Jo, Y. and Wan, K., 2013. Spectral decomposition and reservoir engineering data in mapping thin bed reservoir, Stratton field, South Texas. J. Seismic Explor., 22: 77-91.

Jeffrey, C. and William, J., 1999, On the existence of discrete Wigner distributions. IEEE Signal Process. Lett., 6: 304-306.

Kodera, K., De Villedary, C. and Gendrin, R., 1976. A new method for the numerical analysis of non-stationary signals. Phys. Earth Planet. Inter., 12: 142-150.

Li, C. and Liang, M., 2012. A generalized synchrosqueezing transform for enhancing signal time-frequency representation. Signal Process., 92: 2264-2274.

Liu, W., Cao, S., Liu, Y. and Chen, Y., 2016. Synchrosqueezing transform and its applications in seismic data analysis. J. Seismic Explor., 25: 27-44.

Liu, Y. and Fomel, S., 2013, Seismic data analysis using local time-frequency decomposition. Geophys. Prosp., 61: 516-525.

Oberlin, T., Meignen, S. and Perrier, V., 2014. The Fourier-based synchrosqueezing transform. Acoust., Speech, Signal Process., ICASSP: 315-319.

Oberlin, T., Meignen, S. and Perrier, V., 2015. Second-order synchrosqueezing transform or invertible reassignment? Towards ideal time-frequency representations. IEEE Transact. Signal Process., 63: 1335-1344.

Odebeatu, E., Zhang, J. and Chapman, M., 2006. Application of spectral decomposition to detection of dispersion anomalies associated with gas saturation. The Leading Edge, 25: 206-210.

Partyka, G., Gridley, J. and Lopez, J., 1999, Interpretational application of spectral decomposition in reservoir characterization. The Leading Edge, 22: 353-360.

Radad, M., Gholami, A. and Siahkoohi, H., 2016. A fast method for generating high resolution single-frequency seismic attributes. J. Seismic Explor., 25: 11-25.

Rioul, O. and Vetterlil. M., 1991. Wavelet and signal processing. IEEE Signal Process. Mag., 8: 14-37.

Sinha, S., Routh, P., Anno, P. and Castagna, J.P., 2005. Spectral decomposition of seismic data with continuous-wavelet transform. Geophysics, 70: 19-25.

Thakur, G. and Wu, H.-T., 2011. Synchrosqueezing-based recovery of instantaneous frequencyfrom nonuniform samples. SIAM J. Mathemat. Analys., 43: 2078-2095.

Wu, X., Chapman, M., Wilson, A. and Li, X., 2014. Estimating seismic dispersion from prestack data suing frequency-dependent AVO analysis. J. Seismic Explor., 23: 425-429.